Advances in Technology Innovation, vol. 3, no. 3, 2018, pp. 109 - 117

Effects of Unsteady Aerodynamic Pressure Load in the Thermal Environment of FGM Plates

Chih-Chiang Hong*

Department of Mechanical Engineering, Hsiuping University of Science and Technology, Taichung, Taiwan, ROC.

Received 13 August 2017; received in revised form 14 October 2017; accepted 20 October 2017

Abstract

The effects of unsteady aerodynamic pressure load with varied shear correction coefficient on the functionally graded material (FGM) plates are investigated. Thermal vibration is studied by using the first-order shear deformation theory (FSDT) and the generalized differential quadrature (GDQ) method. Usually, in the FGM analyses, the computed and varied values of shear correction coefficient are the function of the total thickness of plates, FGM power law index, and environment temperature. The effects of environment temperature and FGM power law index on the thermal stress and center deflection of airflow over the upper surface of FGM plates are obtained and investigated. In addition, the effects, with and without the fluid flow over the upper surface of FGM plates, on the center deflection and normal stress are also investigated.

Keywords: aerodynamic pressure, varied shear correction coefficient, FGM, thermal vibration, GDQ

1. Introduction

There are some investigations of aerodynamic pressure load on the functionally graded material (FGM) plates and shells. In 2015, Fazelzadeh et al. [1] studied the effects of volume fraction, aspect ratio and non-dimensional in-plane forces on the nanocomposite FGM plates under the action of supersonic aerodynamic pressure. In 2015, Lee and Kim [2] investigated the structure characteristics of FGM panels under supersonic aerodynamic force. In 2013, Rafiee et al. [3] calculated and studied the nonlinear vibration of piezoelectric FGM shells under combined electrical, thermal, mechanical and aerodynamic loading. In 2012, Ghadimi et al. [4] investigated and studied the thermal flutter characteristics of cantilever FGM plates under supersonic aerodynamic loads. In 2012, Prakash et al. [5] computed and investigated the large amplitude flexural vibration characteristics of FGM plates with supersonic airflow by using the finite element method (FEM). In 2008, Sohn and Kim [6] presented and examined the thermal buckling and flutter characteristics of FGM panels under aero-thermal loads. In 2007, Fazelzadeh and Hosseini [7] studied and investigated a turbo-machinery FGM rotating blades beam under supersonic aero-thermo-elastic loading. In 2007, Wu et al. [8] calculated and analyzed the dynamic stability of FGM plates subjected to aero-thermo-mechanical loads by using the moving least squares differential quadrature method. In 2007, Navazi and Haddadpour [9] investigated the aero-thermo-elastic stability margins of FGM plates and panels in the supersonic flow. In 2006, Prakash and Ganapathi [10] investigated supersonic flutter behavior of FGM plates and flat panels by using the FEM.

There are some computational investigations of generalized differential quadrature (GDQ) in the composited FGM plates and shells. In 2017, Hong [11] investigated the effects of varied shear correction on flutter value of the center deflection and the thermal vibration of FGM shells in an unsteady supersonic flow. In 2015, Tornabene et al. [12] presented a survey of strong formulation FEM focused on the numerical investigation of differential quadrature method. In 2014, Hong [13] studied the thermal vibration and transient response of Terfenol-D FGM plates by using the GDQ method and considering the first-order

* Corresponding author. E-mail address: cchong@mail.hust.edu.tw

shear deformation theory (FSDT) model and the varied modified shear correction factor effects. In 2014, Hong [14] investigated the rapid heating induced vibration of Terfenol-D FGM circular cylindrical shells by using the GDQ method and without considering the effects of shear deformation. In 2013, Hong [15] presented the thermal vibration of Terfenol-D FGM shells by using the GDQ method and also without considering the effects of shear deformation. In 2012, Hong [16] studied the thermal vibration of rapid heating for Terfenol-D FGM plates by using the GDQ method and considering the FSDT effects. In 2009, Tornabene and Viola [17] presented the free vibration analysis of FGM panels and shells by using the GDQ method and considering the FSDT model. It is interesting to study and investigate the thermal stresses and center deflection of GDQ computations by considering the FSDT and the varied effects of the shear correction coefficient of airflow over the upper surface of FGM plates with four edges in simply supported boundary conditions. Environment temperature and FGM power law indextwo parametric effects on the thermal stress and center deflection of airflow over the upper surface of FGM plates are also obtained and investigated. The effects of with and without the fluid flow over the upper surface of FGM plates on the center deflection and normal stress are also calculated.

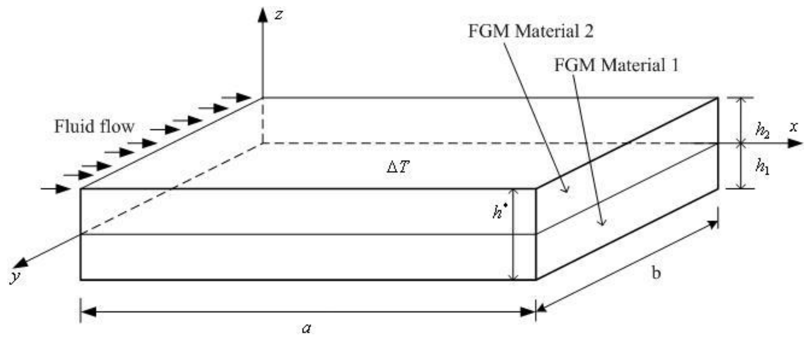

Fig. 1 Fluid flow over the upper surface of two-material FGM plates

2. Formulation

For fluid flow over the upper surface of two-material FGM plates is shown in Fig. 1 with thickness h_1 of FGM material 1 and thickness h_2 of FGM material 2. The material properties are considered in the most dominated property Young's modulus E_{fgm} of FGM with standard variation form of power law index R_n, the others of material properties are assumed in the simple average form [18]. The properties of individual constituent material of FGM are functions of environment temperature T. The time-dependent, linear FSDT equations of displacements u, $v$and w\ of FGM plates are assumed in the following [19].

$$
\begin{aligned}
u &= u^0(x,y,t) + z\psi_x(x,y,t) \\
v &= v^0(x,y,t) + z\psi_y(x,y,t) \\
w &= w(x,y,t)
\end{aligned}
\tag{1}
$$

where u^0 and v^0 are displacements in the x and y axes direction, respectively, w is transverse displacement in the z axis direction of the middle-plane of plates, ψ_x and ψ_y are the shear rotations, t is time.

The normal stresses (σ_x and σ_y) and the shear stresses (σ_{xy}, σ_{yz} andσ_{xz}) in the FGM plate under temperature difference ΔT for the k th layer can be obtained as follows [20-21].

$$
\begin{aligned}
&\begin{Bmatrix} \sigma_x \\ \sigma_y \\ \sigma_{xy} \end{Bmatrix}_{(k)} = \begin{bmatrix} \bar{Q}_{11} & \bar{Q}_{12} & \bar{Q}_{16} \\ \bar{Q}_{12} & \bar{Q}_{22} & \bar{Q}_{26} \\ \bar{Q}_{16} & \bar{Q}_{26} & \bar{Q}_{66} \end{bmatrix}_{(k)} \begin{Bmatrix} \varepsilon_x - \alpha_x \Delta T \\ \varepsilon_y - \alpha_y \Delta T \\ \varepsilon_{xy} - \alpha_{xy} \Delta T \end{Bmatrix}_{(k)} \\
&\begin{Bmatrix} \sigma_{yz} \\ \sigma_{xz} \end{Bmatrix}_{(k)} = \begin{bmatrix} \bar{Q}_{44} & \bar{Q}_{45} \\ \bar{Q}_{45} & \bar{Q}_{55} \end{bmatrix}_{(k)} \begin{Bmatrix} \varepsilon_{yz} \\ \varepsilon_{xz} \end{Bmatrix}_{(k)}
\end{aligned}
\tag{2}
$$

Copyright © TAETI

where α_x and α_y are the coefficients of thermal expansion, α_{xy} is the coefficient of thermal shear, $\bar{Q}_{ij}$ is the stiffness of FGM plates. ε_x, ε_y and ε_{xy} are in-plane strains, not negligible ε_{yz} and ε_{xz} are shear strains. The temperature difference between the FGM plate and curing area is given by the following equation.

$$\Delta T = T_0(x,y,t) + \frac{z}{h^*} T_1(x,y,t) \tag{3}$$

in which T_0 and T_1 are temperature parameters in functions of x, y, and t, h^* is the total thickness of plates.

The dynamic equilibrium differential equations of fluid flow over the upper surface of FGM plates can be represented and obtained in matrix form [15, 21]. In the matrix elements, there are some coefficients (A_{ij}, B_{ij}, D_{ij}), (i,j = 1,2,6), $A_{i^*j^*}$,(i^*, j^* = 4, 5) with partial derivatives of displacements and shear rotations. The external loads are subjected to f_1,..., f_5 with partial derivatives of thermal loads ($\bar{N}$, $\bar{M}$), mechanical loads (p_1, p_2, q) and inertia terms (ρ, H, I). In which (A_{ij}, B_{ij}, D_{ij}), $A_{i^*j^*}$, f_1,..., f_5 and (ρ, H, I) are in the following expressions.

$$\begin{aligned}
f_1 &= \frac{\partial \bar{N}_x}{\partial x} + \frac{\partial \bar{N}_{xy}}{\partial y} + p_1 \\
f_2 &= \frac{\partial \bar{N}_{xy}}{\partial x} + \frac{\partial \bar{N}_y}{\partial y} + p_2 \\
f_3 &= q = \frac{\rho_\infty U_\infty^2}{M_\infty} \frac{\partial w}{\partial x}\bigg|_{z=h^*/2} + \frac{\rho_\infty U_\infty}{M_\infty} \frac{\partial w}{\partial t}\bigg|_{z=h^*/2} \\
f_4 &= \frac{\partial \bar{M}_x}{\partial x} + \frac{\partial \bar{M}_{xy}}{\partial y} \\
f_5 &= \frac{\partial \bar{M}_{xy}}{\partial x} + \frac{\partial \bar{M}_y}{\partial y}
\end{aligned} \tag{4}$$

,

$$\begin{aligned}
(\bar{N}_x, \bar{M}_x) &= \int_{-\frac{h^*}{2}}^{\frac{h^*}{2}} (\bar{Q}_{11}\alpha_x + \bar{Q}_{12}\alpha_y + \bar{Q}_{16}\alpha_{xy}) \Delta T(1,z) dz \\
(\bar{N}_y, \bar{M}_y) &= \int_{\frac{-h^*}{2}}^{\frac{h^*}{2}} (\bar{Q}_{12}\alpha_x + \bar{Q}_{22}\alpha_y + \bar{Q}_{26}\alpha_{xy}) \Delta T(1,z) dz \\
(\bar{N}_{xy}, \bar{M}_{xy}) &= \int_{\frac{-h^*}{2}}^{\frac{h^*}{2}} (\bar{Q}_{16}\alpha_x + \bar{Q}_{26}\alpha_y + \bar{Q}_{66}\alpha_{xy}) \Delta T(1,z) dz \\
(A_{ij}, B_{ij}, D_{ij}) &= \int_{\frac{-h^*}{2}}^{\frac{h^*}{2}} \bar{Q}_{ij}(1, z, z^2) dz, \ (i, j = 1, 2, 6)
\end{aligned} \tag{5}$$

$$A_{i^*j^*} = \int_{\frac{-h^*}{2}}^{\frac{h^*}{2}} k_\alpha \bar{Q}_{i^*j^*} dz, \ (i^*, j^* = 4, 5) \tag{6}$$

$$(\rho, H, I) = \int_{\frac{-h^*}{2}}^{\frac{h^*}{2}} \rho_0 (1, z, z^2) dz \tag{7}$$

in which k_α is the shear correction coefficient, ρ_0 is the density of ply. The values of k_α are usually functions of h^*, T, and R_n. q is the aerodynamic pressure load for the unsteady, in viscid fluid flow over the upper surface of FGM plate with free stream density ρ_∞, velocity U_∞, and Mach number M_∞.

Copyright © TAETI

The simple forms of $\bar{Q}_{ij}$ and $\bar{Q}_{i^*j^*}$ for FGM plates were introduced by Shen [22] in 2007 and used to calculate normal, shear stresses and A_{ij}. The modified shear correction factor k_α can be derived and obtained directly from the total strain energy principle derivation as follows for the FGM plates [13] by considering the varied value effect of k_α on the plates.

$$k_\alpha = \frac{1}{h^*}\frac{FGMZSV}{FGMZIV} \tag{8}$$

in which the expressions of $FGMZSV$ and $FGMZIV$ are functions of h^*, R_n, the Poisson's ratios ν_{fgm}, the Young's modulus of the FGM constituent materials E_1 and E_2 of the FGM plates, respectively.

The dynamic GDQ discrete equations in matrix notation can be derived and obtained for the dynamic equilibrium differential equations by considering four sides simply supported, fluid flow over the upper surface of FGM plates. The GDQ method was presented by Shu and Richards in 1990 [13, 23-25].

3. Computational results

To study and obtain the GDQ results of varied shear correction coefficient calculations with plates layers in the stacking sequence (0°/0°), under four sides simply supported boundary condition, no in-plane distributed forces ($p_1 = p_2 = 0$) and under the external aerodynamic pressure load (q) of airflow over the upper surface of FGM plates with $\rho_\infty = 0.00000678 lb/in^3$, $U_\infty = 23304 in/s$ and $M_\infty = 2$ at altitude 50,000ft. The following coordinates x_i and y_i for the grid points numbers N and M of FGM plates are used

$$\begin{aligned} x_i &= 0.5\,[1-\cos(\frac{i-1}{N-1}\pi)]a, i = 1, 2, ..., N \\ y_j &= 0.5\,[1-\cos(\frac{j-1}{M-1}\pi)]b, j = 1, 2, ..., M \end{aligned} \tag{9}$$

The displacement and temperature of thermal vibrations are used in time sinusoidal form as follows for a simple case study.

$$\begin{aligned} u &= [u^0(x,y) + z\psi_x(x,y)]\sin(\omega_{mn}t) \\ v &= [v^0(x,y) + z\psi_y(x,y)]\sin(\omega_{mn}t) \\ w &= w(x,y)\sin(\omega_{mn}t) \end{aligned} \tag{10}$$

$$q = \frac{\rho_\infty U_\infty^2}{M_\infty}\frac{\partial w(x,y)}{\partial x}\sin(\omega_{mn}t)\Big|_{z=h^*/2} + \frac{\rho_\infty U_\infty}{M_\infty} w(x,y)\omega_{mn}\cos(\omega_{mn}t)\Big|_{z=h^*/2} \tag{11}$$

$$\Delta T = [T_0(x,y) + \frac{z}{h^*}T_1(x,y)]\sin(\gamma t) \tag{12}$$

And with the temperature parameter in the following simple vibration

$$\begin{aligned} T_0(x,y) &= 0 \\ T_1(x,y) &= \overline{T_1}\sin(\pi x/a)\sin(\pi y/b) \end{aligned} \tag{13}$$

in which ω_{mn} is the natural frequency in mode shape numbers m and n of the plates, γ is the frequency of applied heat flux, $\bar{T}_1$ is the amplitude of temperature.

Copyright © TAETI

The SUS304 (stainless steel) for FGM material 1 and the Si_3N_4 (silicon nitride) for FGM material 2 are used in the numerical GDQ computations. Firstly, the dynamic convergence study of center deflection amplitude w (a/2, b/2) (unit mm) in airflow over the upper surface of FGM plates are obtained in Table 1 by considering the varied effects of shear correction coefficient and with h^* = 1.2 mm, $h_1 = h_2$ = 0.6 mm, $m = n = 1$, R_n =1, k_α = 0.149001, T = 100K, $\overline{T}_1 = 100K$, t = 6s. The error accuracy is 7.2E-05 for the center deflection amplitude of $a / b = 1$, a / h^*=10. The 17×17 grid point can be considered in the good convergence result and treated in the following GDQ computations of time responses for deflection and stress of FGM plates. It might be mentioned that the deformations of plates usually increase with the increasing a / h^* for the cases of non thermal loads. However, in the Table1 shows the absolute values of center deflection for thin a / h^*=100 are much smaller than that for thick a / h^*=10 and 5 due to the phenomenon effect of thermal loads. In the FGM plates ($B_{ij} \neq 0$), varied values of k_α are usually functions of h^*, R_n and T. For a / h^*=10, a / b = 1, h^* from 0.12mm to 2.4 mm, $h_1 = h_2$, calculated values of k_α under T =100K are shown in Table 2, used for the GDQ and shear calculations. For h^* = 0.12mm, values of k_α (from 0.109359 to 1.08902) are increasing with R_n (from 0.1 to 2). For h^* = 1.2mm, values of k_α (from 0.891024E-01 to 0.508881) are increasing with R_n (from 0.1 to 10). For h^* = 2.4mm, values of k_α (from 0.836925E-01 to 0.118029E-02) are small decreasing with R_n (from 0.1 to 10). Usually, the values of k_α are dominantly in the inverse proportion to h^* at a given values of R_n and T, e.g. values of k_α (firstly 0.109359, then 0.891024E-01, finally 0.836925E-01) are decreasing with h^* (from 0.12mm, then 1.2mm to 2.4mm) at R_n = 0.1 and T=100K.

Table 1 Dynamic convergence of airflow over the upper surface of FGM plates

a / h^*	GDQ method	Deflection w (a/2, b/2) at t = 6s		
	$N \times M$	a / b = 0.5	a / b = 1	a / b = 2
100	13 × 13	0.166916E-18	-0.864896E-16	-0.113379E-14
	15 × 15	0.166916E-18	-0.864895E-16	-0.113379E-14
	17 × 17	0.166914E-18	-0.864888E-16	-0.113378E-14
14	13 × 13	-0.270625E-14	-0.436330E-12	-0.948251E-10
	15 × 15	-0.270623E-14	-0.436326E-12	-0.947482E-10
	17 × 17	-0.270623E-14	-0.436324E-12	-0.944192E-10
10	13 × 13	-0.190895E-13	-0.318221E-11	-0.674404E-09
	15 × 15	-0.190895E-13	-0.318221E-11	-0.673224E-09
	17 × 17	-0.190893E-13	-0.318244E-11	-0.674404E-09
8	13 × 13	-0.703716E-13	-0.118106E-10	-0.323377E-08
	15 × 15	-0.703718E-13	-0.118357E-10	-0.466268E-08
	17 × 17	-0.703708E-13	-0.118450E-10	-0.595615E-08
5	13 × 13	-0.108713E-11	-0.170468E-09	0.259696E-06
	15 × 15	-0.108830E-11	-0.167507E-09	0.271164E-06
	17 × 17	-0.108713E-11	-0.174309E-09	0.278226E-06

Table 2 Varied shear correction coefficient k_α vs. R_n under T =100K

h^*	k_α						
(mm)	R_n = 0.1	R_n = 0.2	R_n = 0.5	R_n = 1	R_n = 2	R_n = 5	R_n = 10
0.12	0.109359	0.140739	0.288792	0.687883	1.08902	0.989219	0.878104
1.2	0.891024E-01	0.939102E-01	0.111874	0.149001	0.231364	0.415802	0.508881
2.4	0.836925E-01	0.828082E-01	0.815941E-01	0.796610E-01	0.632624E-01	0.219191E-01	0.118029E-02

Secondly, the amplitude of center deflection w (a/2, b/2) (unit mm) for the airflow over the upper surface of FGM plates is calculated. Fig. 2 shows the response values of center deflection amplitude w (a/2, b/2) (unit mm) versus time t in FGM plate for a / h^*=10, 14 and thin a / h^*= 100, respectively, a / b = 1, h^*= 1.2 mm, $h_1 = h_2$= 0.6mm, R_n = 1, k_α = 0.117077, T =653K, $\overline{T}_1$=100K, starting time t = 0.001s and t =0.1s-3.0s with time step is 0.1s. The absolute value of center deflection amplitude is 7.04E-12mm occurs at t = 0.2s, the steady state value of center deflection is -4.54E-12mm for a / h^*=10. The absolute value of center deflection amplitude is 1.31E-12mm occurs at t = 0.1s, the steady state value of center deflection is -6.21E-13mm for a / h^*=14. The absolute values of center deflection for thin a / h^*=100 are much smaller than that for a / h^*=10 and 14.

Copyright © TAETI

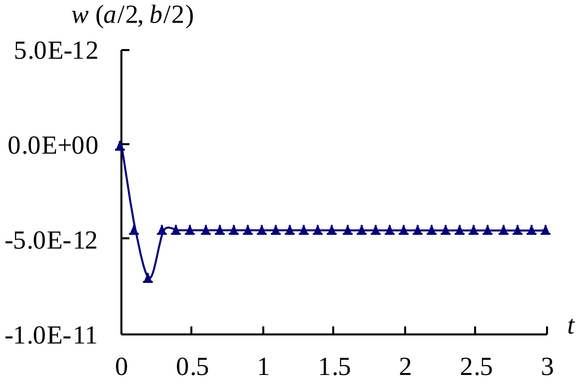

(a) w (a/2, b/2)versus t for a / h^* = 10

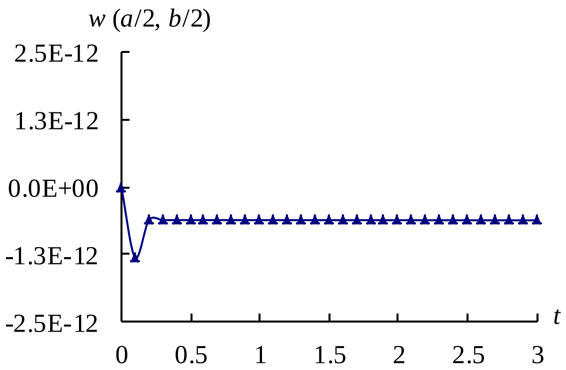

(b) w (a/2, b/2)versus t for a / h^* = 14

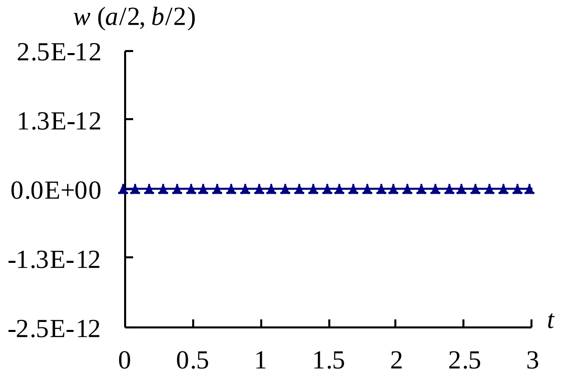

(c) w (a/2, b/2) versus t for a / h^* = 100

Fig. 2 w (a/2, b/2) versus t for a / h^* = 10, 14 and 100

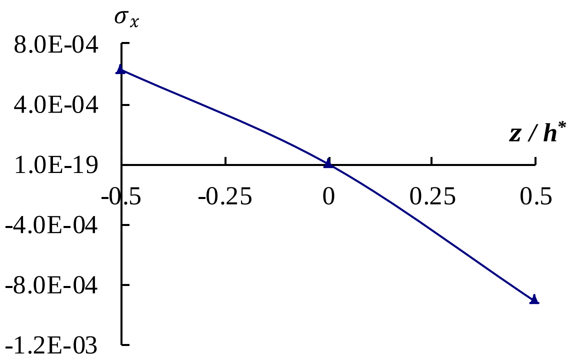

(a) σ_x versus z for a / h^* = 10

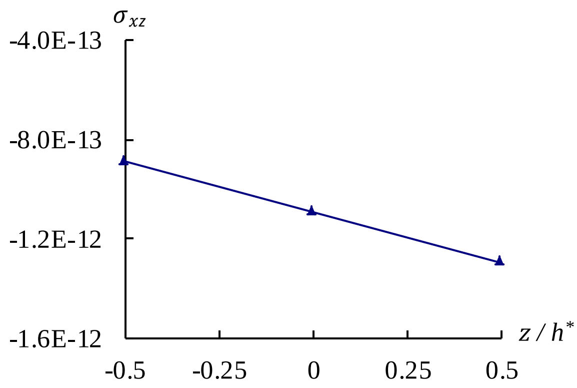

(b) σ_{xz} versus z for a / h^* = 10

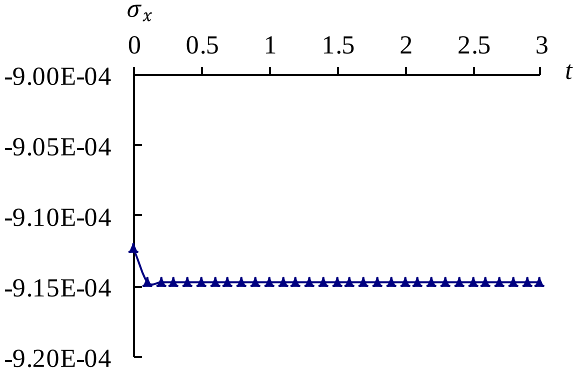

(c) σ_x versus t for a / h^* = 10

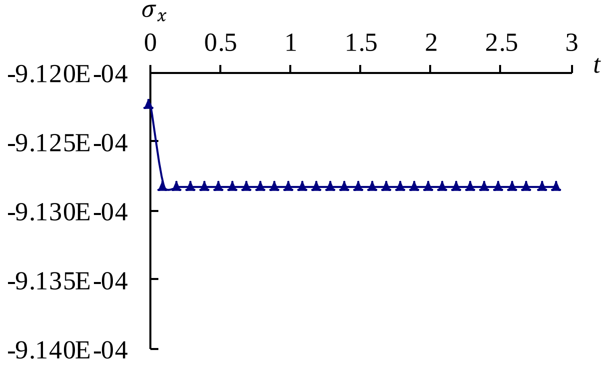

(d) σ_x versus t for a / h^* = 14

Fig. 3 Stresses versus z and t for a / h^* = 10, 14 and 100 (continued)

Copyright © TAETI

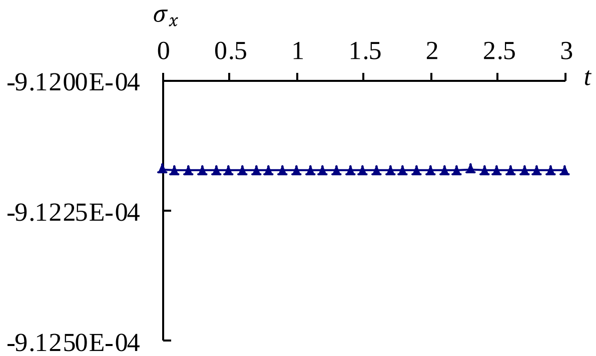

(e) σ_x versus t for $a / h^* = 100$

Fig. 3 Stresses versus z and t for $a / h^* = 10$, 14 and 100

Normal stress σ_x and shear stress σ_{xz} are three-dimensional components and usually in functions of x, y, and z. Typically their values vary through the plate thickness for the airflow over the upper surface of FGM plates. Fig. 3(a) shows the normal stress σ_x (unit GPa) versus z and Fig. 3 (b) shows the shear stress σ_{xz} (unit GPa) versus z at center position ($x = a/2$, $y = b/2$) of plates, respectively at $t = 0.1$s, a / h^*=10 and $a / b = 1$. The absolute value (9.15E-04 GPa) of normal stress σ_x at $z = 0.5h^*$ is found in the much greater value than the value (1.3E-12 GPa) of shear stress σ_{xz} at $z = 0.5h^*$, thus the normal stress σ_x can be treated as the dominated stress for the airflow over the upper surface of FGM plates. Figs. 3(c)-3(e) shows the time responses of the dominated stresses σ_x (unit GPa) at the center position of outer surface $z = 0.5h^*$ as the analyses of deflection case in Fig. 2 for L / h^*=10, 14 and thin L / h^*=100, respectively. The maximum absolute value of stresses σ_x is 9.15E-04 GPa occurs constantly in the periods t =0.2s-3s for L / h^*=10.

Fig. 4 shows the center deflection amplitude $w(a/2, b/2)$ (unit mm) versus T for all different values R_n (from 0.1 to 10) of FGM plates calculated and varied values of k_α, for the airflow over the upper surface of FGM plates $L / h^* = 10$, $a / b = 1$, $h^* = 1.2$ mm, $h_1 = h_2 = 0.6$ mm, $\overline{T}_1 = 100K$, at $t = 3$s. The maximum value of center deflection amplitude is 1.22E-11mm occurs at $T = 653K$ for $R_n = 10$. The center deflection amplitude values are all small, decreasing versus T from $T = 653K$ to $T = 1000K$, for $R_n = 2$, 5 and 10, they can withstand for higher temperature ($T = 1000K$) of environment. The center deflection amplitude values are all small, increasing versus T from $T = 653K$ to $T = 1000K$, for $R_n = 0.1$, 0.2 and 0.5.

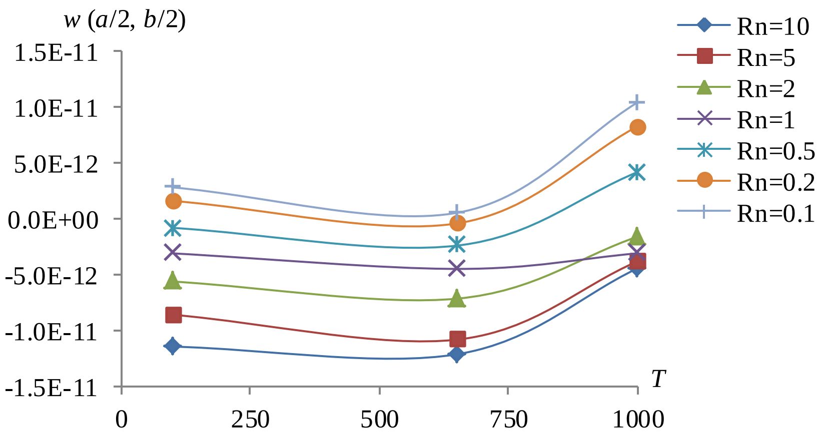

Fig. 4 w (a/2, b/2) versus T

Fig. 5 shows the dominated stresses σ_x (unit GPa) at the center position of outer surface $z = 0.5h^*$ versus T for all different values R_n of FGM plates as the analyses of deflection case in Fig. 4. The absolute values of dominated stresses σ_x versus T are increasing (from $T = 100K$ to $T = 653K$) and then decreasing (from $T = 653K$ to $T = 1000K$) for $R_n = 1$, all decreasing (from $T = 100K$ to $T = 1000K$) for $R_n = 10$, all increasing (from $T = 100K$ to $T = 1000K$) for $R_n = 0.1$, 0.2, 0.5 and 2.

Copyright © TAETI

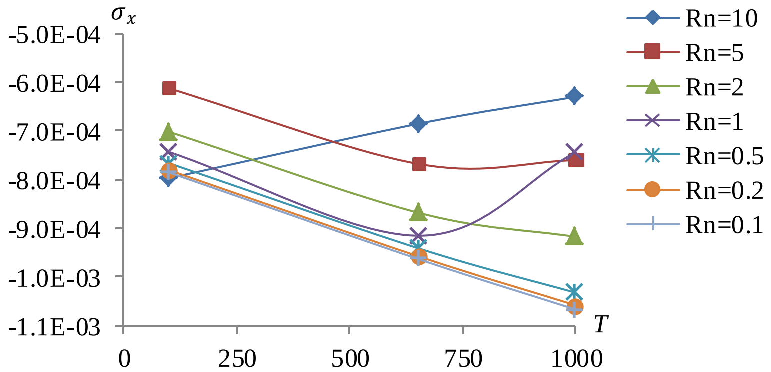

Fig. 5 σ_x versus T

The effects of with and without the fluid flow over the upper surface of FGM plates on the center deflection and normal stress for $a/b=1$, $h^*=1.2$ mm, $h_1=h_2=0.6$ mm, $R_n=1$, $k_\alpha=0.117077$, $T=653K$, $\overline{T_1}=100K$ are also considered as follows. The Fig. 6 (a) shows the response values of center deflection amplitude $w(a/2,b/2)$ (unit mm) versus time t for $a/h^*=10$ with and without airflow over the upper surface of FGM plates. The absolute values of center deflection amplitude for without airflow (0.111079 mm) are much greater than that with airflow (5.26E-14 mm) at t = 0.001s for $a/h^*=10$. Fig. 6 (b) shows the normal stress σ_x (unit GPa) versus z at the center position ($x=a/2, y=b/2$) of plates at t = 0.001s for $a/h^*=10$ with and without airflow over the upper surface of FGM plates. The normal stresses are almost in the same values for with (σ_x=-9.12E-04 GPa at $z=0.5h^*$) and without (σ_x=-9.25E-04 GPa at $z=0.5h^*$) airflow cases.

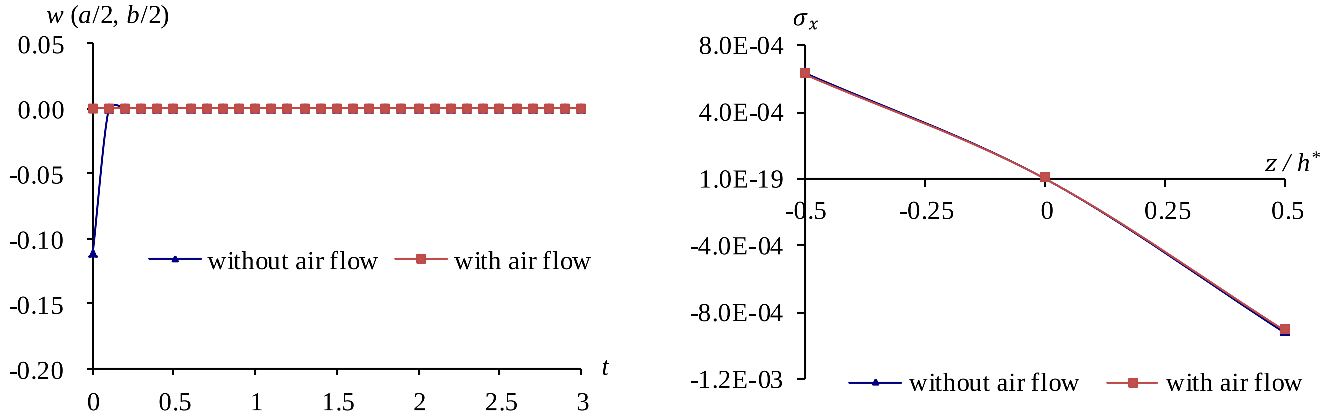

(a) w (a/2, b/2) versus t for a/h^* = 10 (b) w (a/2, b/2) versus t for a/h^* = 10

Fig. 6 w (a/2, b/2) versus t and σ_x versus z for a/h^* = 10 with and without airflow

4. Conclusions

In this study, the GDQ solutions have been obtained and investigated for the deflections and stresses in the thermal vibration of FGM plates by considering the varied effects of shear correction coefficient and the airflow over the upper surface of FGM plates. The GDQ results have shown that varied values of k_α are usually functions of h^*, R_n and T. The absolute value of center deflection amplitude is 7.04E-12 mm occurs at t = 0.2s for $a/h^*=10$ at $T=653K$. The center deflection amplitude values are all small and decreasing versus T from $T=653K$ to $T=1000K$, for R_n = 2, 5 and 10, the FGM plates also can withstand for higher temperature environment.

References

[1] S. A. Fazelzadeh, S. Pouresmaeeli, and E. Ghavanloo, “Aeroelastic characteristics of functionally graded carbon nanotube-reinforced composite plates under a supersonic flow,” Computer Methods in Applied Mechanics and Engineering vol. 285, pp. 714-729, March 2015.

Copyright © TAETI

[2] C. Y. Lee and J. H. Kim, "Evaluation of homogenized effective properties for FGM panels in aero-thermal environments," Composite Structures, vol. 120, pp. 442-450, February 2015.

[3] M. Rafiee, M. Mohammadi, B. S. Aragh, and H. Yaghoobi, "Nonlinear free and forced thermo-electro-aero-elastic vibration and dynamic response of piezoelectric functionally graded laminated composite shells: Part II: Numerical results," Composite Structures, vol. 103, pp. 188-196, September 2013.

[4] M. Ghadimi, M. Dardel, M. H. Pashaei, and M. M. Barzegari, "Effects of geometric imperfections on the aeroelastic behavior of functionally graded wings in supersonic flow," Aerospace Science and Technology, vol. 23, no. 1, pp. 492-504, December 2012.

[5] T. Prakash, M. K. Singha, and M. Ganapathi, "A finite element study on the large amplitude flexural vibration characteristics of FGM plates under aerodynamic load," International Journal of Non-Linear Mechanics, vol. 47, no. 5, pp. 439-447, June 2012.

[6] K. J. Sohn and J. H. Kim, "Structural stability of functionally graded panels subjected to aero-thermal loads," Composite Structures, vol. 82, no. 3, pp. 317-325, February 2008.

[7] S. A. Fazelzadeh and M. Hosseini, "Aerothermoelastic behavior of supersonic rotating thin-walled beams made of functionally graded materials," Journal of Fluids and Structures, vol. 23, no. 8, pp. 1251-1264, November 2007.

[8] L. Wu, H. Wang, and D. Wang, "Dynamic stability analysis of FGM plates by the moving least squares differential quadrature method," Composite Structures, vol. 77, no. 3, pp. 383-394, February 2007.

[9] H. M. Navazi and H. Haddadpour, "Aero-thermoelastic stability of functionally graded plates," Composite Structures, vol. 80, no. 4, pp. 580-587, October 2007.

[10] T. Prakash and M. Ganapathi, "Supersonic flutter characteristics of functionally graded flat panels including thermal effects," Composite Structures, vol. 72, no. 1, pp. 10-18, January 2006.

[11] C. C. Hong, "Effects of varied shear correction on the thermal vibration of functionally-graded material shells in an unsteady supersonic flow," Aerospace, vol. 4, no. 1, pp. 1-15, December 2017.

[12] F. Tornabene, N. Fantuzzi, F. Ubertini, and E. Viola, "Strong formulation finite element method based on differential quadrature: a survey," Applied Mechanics Reviews, vol. 67, no. 2, pp. 1-55, March 2015.

[13] C. C. Hong, "Thermal vibration and transient response of magnetostrictive functionally graded material plates," European Journal of Mechanics - A/Solids, vol. 43, pp. 78-88, January-February 2014.

[14] C. C. Hong, "Rapid heating induced vibration of circular cylindrical shells with magnetostrictive functionally graded material," Archives of Civil and Mechanical Engineering, vol. 14, no. 4, pp. 710-720, August 2014.

[15] C. C. Hong, "Thermal vibration of magnetostrictive functionally graded material shells," European Journal of Mechanics - A/Solids, vol. 40, pp. 114-122, July-August 2013.

[16] C. C. Hong, "Rapid heating induced vibration of magnetostrictive functionally graded material plates," Transactions of the ASME, Journal of Vibration and Acoustics, vol. 134, no. 2, pp. 1-11, January 2012.

[17] F. Tornabene and E. Viola, "Free vibration analysis of functionally graded panels and shells of revolution," Meccanica vol. 44, no. 3, pp. 255-281, June 2009.

[18] S. H. Chi and Y. L. Chung, "Mechanical behavior of functionally graded material plates under transverse load, part I: analysis," International Journal of Solids and Structures, vol. 43, no. 13, pp. 3657-3674, June 2006.

[19] M. S. Qatu, R. W. Sullivan, and W. Wang, "Recent research advances on the dynamic analysis of composite shells: 2000-2009," Composite Structures, vol. 93, no. 1, pp. 14-31, December 2010.

[20] S. J. Lee and J. N. Reddy, "Non-linear response of laminated composite plates under thermomechanical loading," International Journal of Non-Linear Mechanics, vol. 40, no. 7, pp. 971-985, September 2005.

[21] J. M. Whitney, Structural analysis of laminated anisotropic plates, Lancaster: Pennsylvania, USA, Technomic Publishing Company, Inc., 1987.

[22] H. S. Shen, "Nonlinear thermal bending response of FGM plates due to heat condition," Composites Part B: Engineering, vol. 38, no. 2, pp. 201-215, March 2007.

[23] C. Shu and B. E. Richards, "High resolution of natural convection in a square cavity by generalized differential quadrature," Proc. 3rd International Conf. Advanced in numerical Methods in Engineering: Theory and Applications, Swansea, vol. 2, pp. 978-985, 1990.

[24] C. W. Bert, S. K. Jang, and A. G. Striz, "Nonlinear bending analysis of orthotropic rectangular plates by the method of differential quadrature," Computational Mechanics, vol. 5, no. 2-3, pp. 217-226, March 1989.

[25] C. Shu and H. Du, "Implementation of clamped and simply supported boundary conditions in the GDQ free vibration analyses of beams and plates," International Journal of Solids and Structures, vol. 34, no. 7, pp. 819-835, March 1997.

Copyright © TAETI